J|A|C|S COMMUNICATIONS

Published on Web 10/13/2010

Assembly of Modular Asymmetric Organic−Inorganic Polyoxometalate Hybrids into Anisotropic Nanostructures

Mali H. Rosnes,[†] Chiara Musumeci,[‡] Chullikkattil P. Pradeep,[†] Jennifer S. Mathieson,[†] De-Liang Long,[†] Yu-Fei Song,[†] Bruno Pignataro,*[,§] Richard Cogdell,*[,||] and Leroy Cronin*[,†]

WestCHEM, School of Chemistry, University of Glasgow, Joseph Black Building, University Avenue, Glasgow, G12 8QQ, U.K., Superlab - Consorzio Catania Ricerche, S.le Primosole 50, 95121 Catania, Italy, Dipartimento di Chimica Fisica "F. Accascina", Università di Palermo, V.le delle Scienze, Parco D'Orleans II, Ed.17 - 90128 Palermo, Italy, and Glasgow Biomedical Research Centre, University of Glasgow, University Avenue, Glasgow, G12 8QQ, U.K.

Received July 26, 2010; E-mail: L.Cronin@chem.gla.ac.uk; r.cogdell@bio.gla.ac.uk; bruno.pignataro@unipa.it

Ⓦ **This paper contains enhanced objects available on the Internet at http://pubs.acs.org/jacs.**

Abstract: Three organic−inorganic hybrid Mn-Anderson polyoxometalates (POMs), with both symmetrical and asymmetrical appended groups, have been synthesized, identified using electrospray mass spectrometry, and isolated using an approach that allows the three AA, BB, and AB compounds to be structurally characterized. Investigation of the self-assembly of the hybrids on hydrophilic surfaces reveals the formation of nanofibres with characteristics that reflect the nature of the substitution of the POM yielding a route to the programmed assembly of anisotropic hybrid nanostructures.

Polyoxometalates (POMs) are metal-oxide clusters of early transition metals Mo, W, V, etc.[1] with a seemingly endless structural versatility and a wide range of properties,[2] which can be further optimized and developed by the design of organic−inorganic hybrids.[3] However the design of hybrids that can be 'programmed'[4] to self-assemble into anisotropic structures on surfaces are not yet known.[5] To address this gap, we have been working with the Mn-Anderson anion cluster archetype, $[MnMo_6O_{24}H_6]^{3-}$, which can be grafted with tris(hydroxymethyl)methane (TRIS) based organic groups on either side of the Anderson-cluster 'platform,' and this has been used widely in the generation of symmetrical hybrid architectures.[6] We opted to use the Anderson cluster because we reasoned that asymmetrically ligated clusters (i.e., with different functionalities on either side) should be interesting from a self-assembly point of view. However, the synthesis and isolation of such asymmetric Mn-Anderson hybrid clusters is not trivial.[7] This is because the synthetic approach, involving the Mn-Anderson cluster and two TRIS based organic functionalities, could result in three statistically controlled products in the reaction mixture [AA, AB (=BA), BB].

Here we have specifically targeted a modular synthetic approach which leads to the generation of three Mn-Anderson based hybrid POMs with an asymmetric Mn-Anderson cluster $TBA_3[(MnMo_6O_{18})((OCH_2)_3C-C_9H_{17})((OCH_2)_3CNH-CH-C_{16}H_9)]$ (**1**) containing different ligands on either side of the cluster anion and two symmetric Mn-Anderson clusters having identical ligands on either side of the Mn-Anderson cluster $TBA_3[(MnMo_6O_{18})((OCH_2)_3C-C_9H_{17})_2]$ (**2**) and $TBA_3[(MnMo_6O_{18})((OCH_2)_3CNH-CH_2-C_{16}H_9)_2]$ (**3**)[8] (where TBA = tetrabutylammonium cation) in a one pot reaction. Further, by employing the Langmuir−Blodgett (LB) technique, we demonstrate that these constitute unique building blocks for the fabrication of hierarchical anisotropic nanostructures. This is interesting since the two TRIS-based organic functionalities grafted onto the Mn-Anderson cluster include a highly conjugated aromatic moiety ($(HOCH_2)_3CNH-CH_2-C_{16}H_9 = H_3L^1$),[8] which is used to modify the properties of the Anderson metal oxide cluster, as well as allowing the cluster to assemble exploiting aromatic $\pi-\pi$ interactions, and a C_9 alkyl chain with an unsaturated end group ($(HOCH_2)_3C-C_9H_{17} = H_3L^2$)[9] which could control the self-assembly behavior of clusters on surfaces. Importantly, the self-assembly behavior of these hybrids are found to depend on the grafted organic functionalities L^1 and L^2, and two compounds are capable of assembling into unique anisotropic nanostructures on hydrophilic silicon surfaces.

The typical synthetic approach employed trying to achieve the products **1** and **2** involves the reaction of equal amounts of the organic functionalities H_3L^1 (0.437 g, 1.3 mmol) and H_3L^2 (0.300 g, 1.3 mmol) in 45 mL of dry acetonitrile under reflux at 80 °C for 16 h with $(TBA)_4[\alpha\text{-}Mo_8O_{26}]$ (1.618 g, 0.75 mmol) and $Mn(OAc)_3 \cdot 2H_2O$ (0.305 g, 1.14 mmol). The orange/brown reaction mixture was then cooled to room temperature. After cooling, toluene is then added to the mother liquor to enable slow crystallization by evaporation of the solvent mixture. In this way, the precipitation

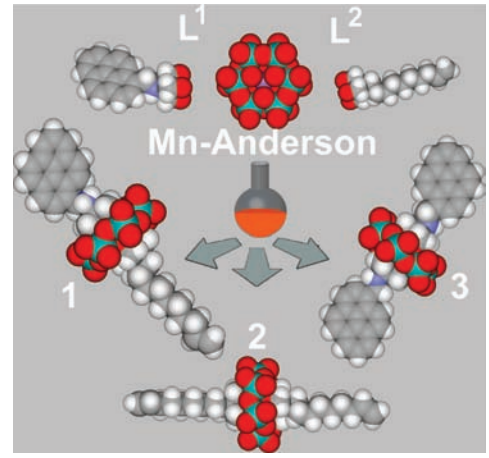

Figure 1. A schematic presentation of the one pot reaction with the three possible outcomes. Each of the compounds **1**−**3** are −3 anions.

[†] WestCHEM, University of Glasgow.
[‡] Superlab - Consorzio Catania Ricerche.
[§] Università di Palermo.
[||] Glasgow Biomedical Research Centre, University of Glasgow.

 10.1021/ja1066338

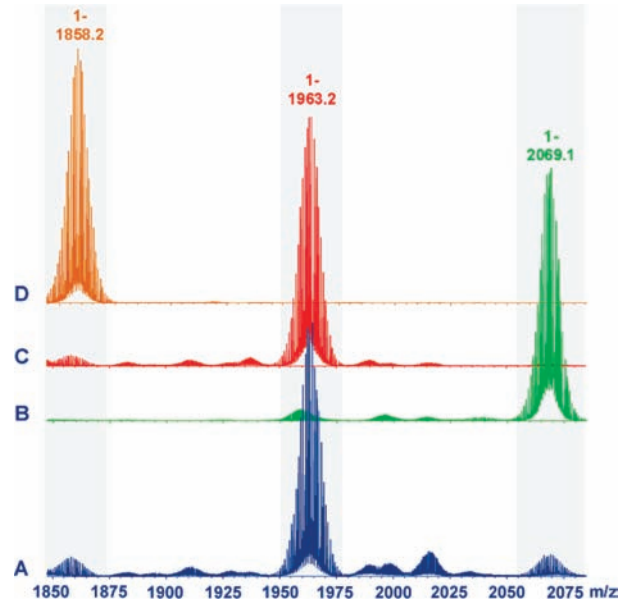

Figure 2. The mass spectrum labeled A (blue) was performed on the mother liquor before crystallization and shows a mixture of the three possible compounds **1**, **2**, and **3**. By means of comparison the mass spectra for samples of the pure compounds **1**, **2**, and **3** are shown in spectra C (red), D (orange), and B (green) respectively. In spectrum A the intensity ratio between the peak at 1963.2 (compound **1**) to the peak at 1858.2 (compound **2**) is 12:1, while in the purified spectrum C it is 22:1.

occurs from the mother liquor, where products **1**, **2**, and **3** can be obtained which were characterized by elemental analysis, IR, NMR, UV−vis, ESI-MS, TGA-DSC, and finally single crystal X-ray crystallography (see Supporting Information (SI) for details). However it should be noted that this procedure is optimal for the synthesis of the asymmetric cluster, **1**, giving a 14% yield. To synthesize **2**, a modified procedure using only H_3L^2 is employed giving the product in 75% yield. In both cases crystals suitable for single crystal X-ray analyses were grown from solutions of dimethylformamide by ether diffusion. Figure 1 depicts the connectivity of the structures of the three hybrid molecular cluster anion units, as determined by X-ray crystallography for compounds **1** and **2** and presented previously for compound **3**.[8]

Most importantly, we were able to successfully follow the assembly of the hybrid clusters using electrospray ionization mass spectrometry (ESI-MS), and this approach helped us establish our modular synthesis; see Figure 2.[7] This was the key technique that allowed us to observe the assembly of the symmetrical compounds **2** and **3**, as well as the asymmetric compound **1**, and also allowed us to screen different compound batches which were separated by selective precipitation. Therefore the mass spectrometry studies allowed us to confirm the presence of each of the compounds and devise strategies to their isolation and purification.

To investigate the potential of these compounds to assemble on surfaces, LB films of compounds **1**−**3** were transferred at relatively low pressures (10 mN/m) and at 25 °C from the air/water interface to hydroxylated silicon surfaces (Si−OH). Under these conditions, dynamic Scanning Force Microscopy (SFM) revealed a unique self-assembly behavior[10] of compounds **1** and **3** showing the formation of nanoscopic fibers with laterally organized and ordered superstructures[11] closely resembling biological fibrils; see Figures 3 and 4 and video depicting a cartoon of the possible assembly process. In particular, highly ordered and stable (up to 6 months) POM nanofibers were observed for the asymmetric Anderson cluster (**1**) containing L^1 and L^2. Compound **3** containing L^1 grafted on either

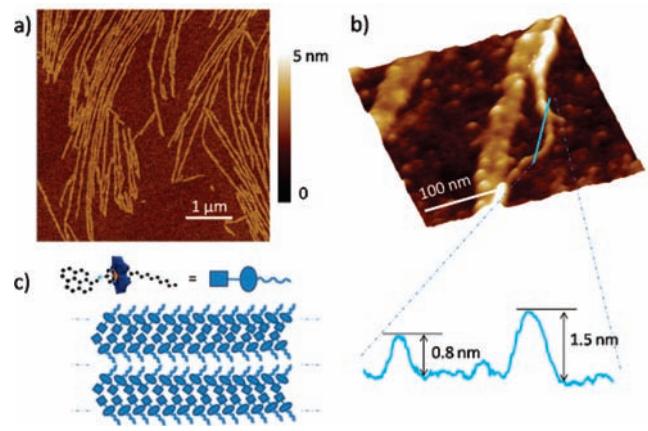

Figure 3. LB submonolayer of **1** on Si−OH: (a) SFM large scale image; (b) zoom in a region of (a) with a section profile along the marked line; (c) cartoon showing the suggested hierarchical arrangement of **1** into fibrils.

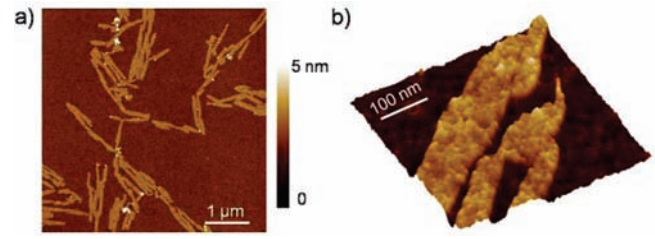

Figure 4. LB submonolayer of **3** on Si−OH: (a) SFM large scale image; (b) zoom in a restricted region of (a) showing short and large fibrils.

side of the cluster is also found to form laterally organized nanofibers, but with different dimensional features. Compound **2** with two L^2 did not form fibers under these conditions (see SI), and Figure 3b shows a close-up of the fibers formed from compound **1**, which also shows that they tend to organize into bidimensional fibril-like structures. This process shows in turn a type of hierarchical organization where hybrid POMs at first form 1D fibers that then go on to assemble to form 2D superstructures of these fibers.

The sizes of these structures revealed by section analysis, in combination with the X-ray structures of the compounds, can help give us insight into the mechanism of self-assembly. This is because compound **1** forms regular fibrils 1−5 μm long, 60−70 nm wide, and about 0.8 nm tall, their height closely resembling the diameter of an individual cluster core. Individual fibers disconnected by a fibril are observed in Figure 3b.

These fibers are about 0.8 nm tall (note also the presence of fiber crossing points with double the height), and their lateral size typically measures less than 20 nm. By considering the well-known SFM tip-broadening effect (see SI), this lateral size is consistent with one set (or at most a few) of laterally paired POM-hybrid molecules. A comparison of the above findings with crystallographic data (as shown in Figure 5) allows us to postulate a mode of fiber growth in Figure 3c. This describes the assembly of L^1 units through $\pi-\pi$ stacking interactions between two adjacent hybrid cluster units on the surface.

For compound **3**, containing two aromatic L^1 ligands, we also observe the formation of fibril-like systems showing the same height range, but these are typically shorter (0.2−1 μm) and wider (about 130 nm) than the case for compound **1**; see Figure 4. The fact that only the pyrene containing compounds **1** and **3** form fibers at the interfacial surface points to the importance of the aromatic L^1 moiety for anisotropic growth. At the same time, the presence of the L^2 is also crucial in controlling the growth mode, allowing for an

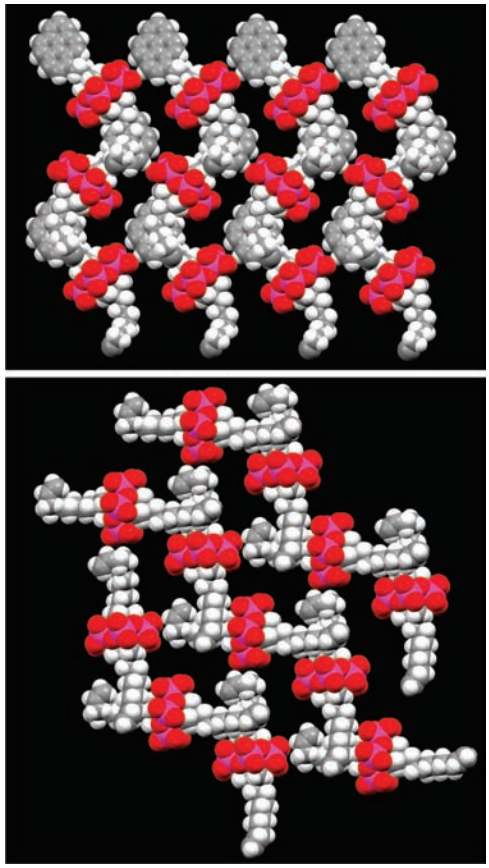

Figure 5. A packing diagram of the hybrid cluster anions found in compound **1** (top) and compound **2** (bottom) with the atoms shown in space-filling mode. The solvent, disordered parts, and TBA cations have been omitted for clarity. C, gray; H, white; Mo, purple; O, red.

increased aspect ratio of the fibrils, which is about 30:1 (length: width) for compound **1** compared to about 6:1 for compound **3**. In addition to the weaker interaction between the aliphatic tails, the above effect is probably due to a decrease of entropy due to the ordering of long interacting organic tails.

To better understand the possible process of self-assembly on the surfaces, it is worth considering the 3D solid state crystal structures of compounds **1**, **2**, and **3** which have been determined by single crystal X-ray crystallographic analysis, and the packing motifs for compounds **1** and **2** are shown in Figure 5 (the structure of **3** has been presented previously; see ref 8). Similar to compound **3**, the hybrid cluster anions found in compound **1** are found to associate via C−H···O═Mo hydrogen-bond-like interactions in the range of *ca.* 2.2−2.7 Å and orientate the pyrene 'head' groups (Figure 5, top view) so they are adjacent to each other with the hydrophobic tail groups suspended also so they are adjacent to one another forming a layered structure. The hybrid cluster anion found in compound **2**, by contrast, forms a grid-like structure with the long chains packing in a criss-cross manner whereby adjacent carbon chains fold over one another (Figure 5, bottom).

Therefore, taking into account these structural considerations it is possible to imagine that the hybrid asymmetric cluster anion could form fibers with higher aspect ratios due to the formation of a type of layered structure whereby the pyrene 'head' groups are organized by a combination of pyrene−pyrene $\pi-\pi$ and pyrene-cluster C−H···O═Mo interactions on one side, with the hydrophobic interactions of the interdigitated carbon chains on the other (see Figure 3c). As such we could tentatively suggest that the cluster-hybrid anions found in compound **3** are therefore less efficiently packed together on the surface forming fibers with increased lateral interaction along with fiber pairing, sudden turns, and sharp angles in the superstructures formed. Finally this model would mean that the pyrene head groups are required for fiber formation, and this is at least consistent with the fact that the hybrid cluster anions found in compound **2** do not form fibers under the same conditions as those for compounds **1** and **3**.

In conclusion, we have achieved the synthesis, separation, and crystal structure determination of symmetric and asymmetric polyoxometalate (POM) Mn-Anderson based hybrid clusters, including a novel asymmetric organic−inorganic hybrid POM having two different appended organic functionalities. The assembly of these structures shows protein-like fribril architectures on surfaces leading to high aspect ratio anisotropic nanostructures due to the interactions between the aromatic and aliphatic moieties. In future work we will explore the self-assembly by varying the cation, cluster type, and also investigating the influence of patterned substrates on the fibril formation.

Acknowledgment. We thank the EPSRC, WestChem, NSF, A. P. Sloan Foundation, and Lord Kelvin and Adam Smith Scholarship. This work was supported by the Italian MiUR (PRIN 2009, FIRB "Futuro in Ricerca") and University of Palermo.

Supporting Information Available: Experimental details, crystallographic data, and video clip. This material is available free of charge via the Internet at http://pubs.acs.org.

References

(1) Long, D. L.; Burkholder, E.; Cronin, L. *Chem. Soc. Rev.* **2007**, *36*, 105–121. Pope, M. T.; Müller, A. *Angew. Chem., Int. Ed.* **1991**, *30*, 34–48.
(2) Hill, C. L. *Chem. Rev.* **1998**, *98*, 1–2. Long, D. L.; Tsunashima, R.; Cronin, L. *Angew. Chem., Int. Ed.* **2010**, *49*, 1736–1758.
(3) Proust, A.; Thouvenot, R.; Gouzerh, P. *Chem. Commun.* **2008**, 1837–1852. Gouzerh, P.; Proust, A. *Chem. Rev.* **1998**, *98*, 77–111.
(4) Pradeep, C. P.; Long, D. L.; Newton, G. N.; Song, Y. F.; Cronin, L. *Angew. Chem., Int. Ed.* **2008**, *47*, 4388–4391. Fleming, C.; Long, D. L.; McMillan, N.; Johnston, J.; Bovet, N.; Dhanak, V.; Gadegaard, N.; Kögerler, P.; Cronin, L.; Kadodwala, M. *Nat. Nanotechnol.* **2008**, *3*, 229–233.
(5) Bu, W. F.; Li, H. L.; Sun, H.; Yin, S. Y.; Wu, L. X. *J. Am. Chem. Soc.* **2005**, *127*, 8016–8017.
(6) Allain, C.; Favette, S.; Chamoreau, L. M.; Vaissermann, J.; Ruhlmann, L.; Hasenknopf, B. *Eur. J. Inorg. Chem.* **2008**, 3433–3441. Favette, S.; Hasenknopf, B.; Vaissermann, J.; Gouzerh, P.; Roux, C. *Chem. Commun.* **2003**, 2664–2665. Song, Y. F.; McMillan, N.; Long, D. L.; Kane, S.; Malm, J.; Riehle, M. O.; Pradeep, C. P.; Gadegaard, N.; Cronin, L. *J. Am. Chem. Soc.* **2009**, *131*, 1340–1341.
(7) Song, Y. F.; Long, D. L.; Kelly, S. E.; Cronin, L. *Inorg. Chem.* **2008**, *47*, 9137–9139.
(8) Song, Y. F.; Long, D. L.; Cronin, L. *Angew. Chem., Int. Ed.* **2007**, *46*, 3900–3904.
(9) Muth, A.; Asam, A.; Huttner, G.; Barth, A.; Zsolnai, L. *Chem. Ber.* **1994**, *127*, 305–311.
(10) Drop casting on the same substrate does not lead to the above 1D systems, indicating that the air/water interface plays a crucial role in preorienting the POM building blocks for self-assembling.
(11) Pignataro, B. *J. Mater. Chem.* **2009**, *19*, 3338–3350.

JA1066338